Cell

The AAA+ ATPase Thorase Regulates AMPA Receptor-Dependent Synaptic Plasticity and Behavior

Jianmin Zhang,[1,2] Yue Wang,[7] Zhikai Chi,[2,3] Matthew J. Keuss,[1,6] Ying-Min Emily Pai,[1,2] Ho Chul Kang,[1,2] Joo-ho Shin,[1,2] Artem Bugayenko,[1,2] Hong Wang,[3] Yulan Xiong,[1,2] Mikhail V. Pletnikov,[2,5] Mark P. Mattson,[3,7] Ted M. Dawson,[1,2,3,*] and Valina L. Dawson[1,2,3,4,*]

[1]Neuroregeneration and Stem Cell Programs, Institute for Cell Engineering
[2]Department of Neurology
[3]Solomon H. Snyder Department of Neuroscience
[4]Department of Physiology
[5]Department of Psychiatry and Behavioral Sciences
Johns Hopkins University School of Medicine, Baltimore, MD 21205, USA
[6]Department of Chemical and Biomolecular Engineering, Johns Hopkins University, Baltimore, MD 21205, USA
[7]Laboratory of Neurosciences, National Institute on Aging Intramural Research Program, Baltimore, MD 21224, USA
*Correspondence: tdawson@jhmi.edu (T.M.D.), vdawson@jhmi.edu (V.L.D.)
DOI 10.1016/j.cell.2011.03.016

SUMMARY

The synaptic insertion or removal of AMPA receptors (AMPAR) plays critical roles in the regulation of synaptic activity reflected in the expression of long-term potentiation (LTP) and long-term depression (LTD). The cellular events underlying this important process in learning and memory are still being revealed. Here we describe and characterize the AAA+ ATPase Thorase, which regulates the expression of surface AMPAR. In an ATPase-dependent manner Thorase mediates the internalization of AMPAR by disassembling the AMPAR-GRIP1 complex. Following genetic deletion of *Thorase*, the internalization of AMPAR is substantially reduced, leading to increased amplitudes of miniature excitatory postsynaptic currents, enhancement of LTP, and elimination of LTD. These molecular events are expressed as deficits in learning and memory in Thorase null mice. This study identifies an AAA+ ATPase that plays a critical role in regulating the surface expression of AMPAR and thereby regulates synaptic plasticity and learning and memory.

INTRODUCTION

The excitatory amino acid glutamate plays important roles in neuronal development, synaptic plasticity, and neurodegeneration through activation of N-methyl-D-aspartate (NMDA) receptors and α-amino-3-hydroxy-5-methylisoxazole-4-proprionate (AMPA) receptors (AMPAR) (Besancon et al., 2008; Kessels and Malinow, 2009). Synaptic strength is thought to be determined, in part, through the activity-dependent insertion and endocytosis of AMPAR (Kessels and Malinow, 2009), which regulate long-term potentiation (LTP) and long-term depression (LTD), and the initiation and formation of long-lasting memories (Kessels and Malinow, 2009). AMPAR are ionophores composed of a heteromeric complex of combinations of GluR1 through GluR4 subunits. A number of intracellular proteins regulate the trafficking of AMPAR, thereby regulating neuronal excitability (Kessels and Malinow, 2009; Shepherd and Huganir, 2007).

The C-terminal PDZ-binding domain of GluR2 receptors is important in AMPAR internalization by binding proteins such as glutamate receptor-interacting protein (GRIP1) and protein interacting with C-kinase-1 (PICK1) (Dong et al., 1997; Hanley, 2008; Shepherd and Huganir, 2007). Clathrin adaptor AP2, small GTPase Rab5, Homer, CPG2, dynamin 3, and Arc/Arg3.1 are also involved in controlling AMPAR endocytosis as is GluR1 AMPAR phosphorylation. These studies have provided insight into the protein machinery involved in AMPAR trafficking (Kessels and Malinow, 2009; Newpher and Ehlers, 2008; Sheng and Hoogenraad, 2007; Shepherd and Huganir, 2007). However, the specific mechanisms of AMPAR internalization are not well understood.

Here we describe and characterize neuroprotective gene 6 (*NPG6*) (EF688601), currently annotated as *Atad1*, which we named *Thorase* after Thor, the Norse God of Thunder and Lightening (Dai et al., 2010). Thorase controls AMPAR internalization in an ATPase-dependent manner by disassembling GluR2 and GRIP1 complexes. In the absence of Thorase, the internalization of AMPAR is decreased, leading to increased amplitude of miniature excitatory postsynaptic currents, enhanced LTP, and impaired expression of LTD. These physiologic outcomes result in deficits in learning and memory. These results define an ATPase-dependent process that regulates the intracellular trafficking of AMPAR.

RESULTS

Thorase Is an AAA$^+$ ATPase

Thorase is a 361 amino acid protein (Figure S1A available online) containing an AAA ATPase domain composed of Walker A (ATP-binding motif) and Walker B (ATP hydrolysis motif) motifs, similar to other ATPases (Figure S1B). Consistent with general ATPase structures, Thorase contains an N-linker (NL) domain, which may transduce energy from ATP hydrolysis to the rest of the protein, and a second region of homology (SRH) that differentiates classically defined AAA proteins from the broader AAA$^+$ family (White and Lauring, 2007) (Figure 1A and Figure S1A). Thorase possesses ATPase activity with a Michaelis-Menten constant (K_M) of 43.4 μM and a V_{max} of 11.0 nM ATP/min/mg protein (Figures 1B and 1C). The ATPase activity of the Walker A (K193T) (mA-Thorase) mutant or the Walker B (E139Q) (mB-Thorase) mutant is reduced by 60%–70% or by greater than 92% in the mutant containing both mutations (mAB-Thorase) (Figure 1C).

Expression Pattern and Synaptic Enrichment of Thorase in Mouse Brain

Northern blot analysis shows that Thorase mRNA is expressed in many tissues with the highest expression in the brain and testes (Figure S1C). Polyclonal and monoclonal antibodies to Thorase recognize a single band on immunoblot analysis that is not present in Thorase gene-deleted tissues (Figure S1D, see Figure S2D). Immunoblot analysis reveals a heterogeneous expression of Thorase in mouse brain (Figures S1E and S1F). Immunohistochemistry shows heterogeneous expression of Thorase with relatively high expression in hippocampal CA1 pyramidal cells (Figures S1G–S1J).

Subcellular fractionation from whole mouse brain shows that Thorase segregates into the P2 fraction (crude synaptosome) but not in the P1 (nucleus) or the S2 (cytosol) fractions. Within the P2 fraction, Thorase segregates to the LP1 fraction (synaptosomal membranes) with minor segregation in the P3 (light membranes) and LP2 (synaptic vesicle-enriched fraction), and none in the S3 (cytosol) and LS2 (synaptic cytosol) (Figure 1D). The subcellular distribution of Thorase was compared to the synaptic proteins: GRIP1, GluR1, GluR2, postsynaptic density protein 95 (PSD95), vesicle-associated membrane protein 2 (VAMP2), α-synuclein, and synaptophysin 1. Histone was used as a nuclear marker and phosphoglycerate kinase 1 (PGK1) was used as a cytosolic marker (Figure 1D). The enrichment of these proteins in their respective fractions indicates that the fractionation was effective. Thorase cosegregates with the postsynaptic proteins PSD95, GRIP1, GluR1, and GluR2 in the LP1 fraction (Figure 1D). To investigate the localization of Thorase with synaptic proteins, primary mouse hippocampal neurons were costained with Thorase monoclonal antibodies and synaptic marker antibodies. By confocal microscopy, Thorase colocalizes with the postsynaptic marker PSD95 (Figures 1E and 1F) and the AMPARs GluR1 and GluR2 (Figures 1G and 1H), whereas it is juxtaposed to the presynaptic marker synapsin 1. Coimmunostaining of Thorase and the axon-specific marker SMI312 shows that Thorase is not expressed in axons (Figure S1K). Coexpression of Thorase with postsynaptic proteins in HEK293 cells followed by coimmunoprecipitation indicates that Thorase specifically interacts with GRIP1 but fails to coimmunoprecipitate with GRIP2, Arc, Homer 1, Homer 2, PICK1, and PSD95 (Figure 1I). Domain mapping via coimmunoprecipitation experiments in HEK293 cells with Thorase and different PDZ domains of GRIP1 indicates that Thorase interacts with the PDZ5 domain of GRIP1 (Figure 1J). Coimmunoprecipitation experiments indicate that Thorase also binds to GluR2 (Figure 1K). GST-pull down of Thorase with different C-terminal truncations of GluR2 indicates that Thorase interacts with amino acids 832–839 of the C terminus of GluR2 (Figure 1L). Thorase also interacts with GluR2 and GRIP in vivo (see Figure 5). These results taken together indicate that Thorase is a postsynaptic enriched protein that colocalizes with AMPAR and interacts with both GRIP1 and GluR2.

Thorase Overexpression Decreases Surface AMPAR and AMPA Currents

To explore the possibility that Thorase could regulate AMPAR surface expression in an ATPase-dependent manner, wild-type (WT) Thorase or the Thorase ATPase-deficient Walker AB mutant (mAB-Thorase) with or without a GFP-tag (Figures S1L and S1M) were overexpressed in high-density mouse cortical and hippocampal neural cultures via lentiviral transduction. Expression of Thorase with or without the GFP-tag decreases the level of surface GluR2 AMPAR as revealed by a surface biotinylation assay, whereas mAB-Thorase has no effect (Figures 1M and 1N). Expression of Thorase-GFP leads to a 28.1% reduction in surface GluR2 receptor intensity in low-density mouse hippocampal neurons by live-cell immunohistochemistry with an anti-GluR2 N-terminal antibody compared to GFP control cultures (Figures 1O and 1P). Overexpression of mAB-Thorase-GFP has no effect on surface GluR2 expression compared to GFP control (Figures 1O and 1P). Adult mice were stereotaxically injected with lenti-GFP, lenti-Thorase-GFP, or lenti-mAB-Thorase-GFP virus into the hippocampi. One week later hippocampal slices were prepared and NMDA and AMPA currents were recorded at 40 mV and −70 mV in GFP-positive neurons (see Figure 6). NMDA currents are not affected by Thorase-GFP overexpression, but AMPA currents are reduced by 20% compared to GFP controls (Figures 1Q and 1R). mAB-Thorase-GFP expression shows no effect on either NMDA or AMPA currents (Figures 1Q and 1R). Taken together these results suggest that Thorase specifically regulates AMPAR surface expression in an ATPase-dependent manner both in vitro and in vivo.

Generation of Conditional Thorase Knockout Mice

Conditional Thorase knockout (KO) mice were generated by flanking exon 5 and exon 6 containing the AAA Walker A and Walker B domains with *loxP* sites (Figure S2A). Genomic deletion of *Thorase* was achieved by breeding to male germline Protamine-Cre deletor mice. Southern blot analysis confirms the successful targeting with a 9.3 kb WT band and an 11.8 kb targeted band (Figure S2B). PCR confirms the KO of Thorase (Figure S2C). Immunoblot analysis and immunohistochemistry with a Thorase-specific C-terminal antibody (see Figure S1D) reveals

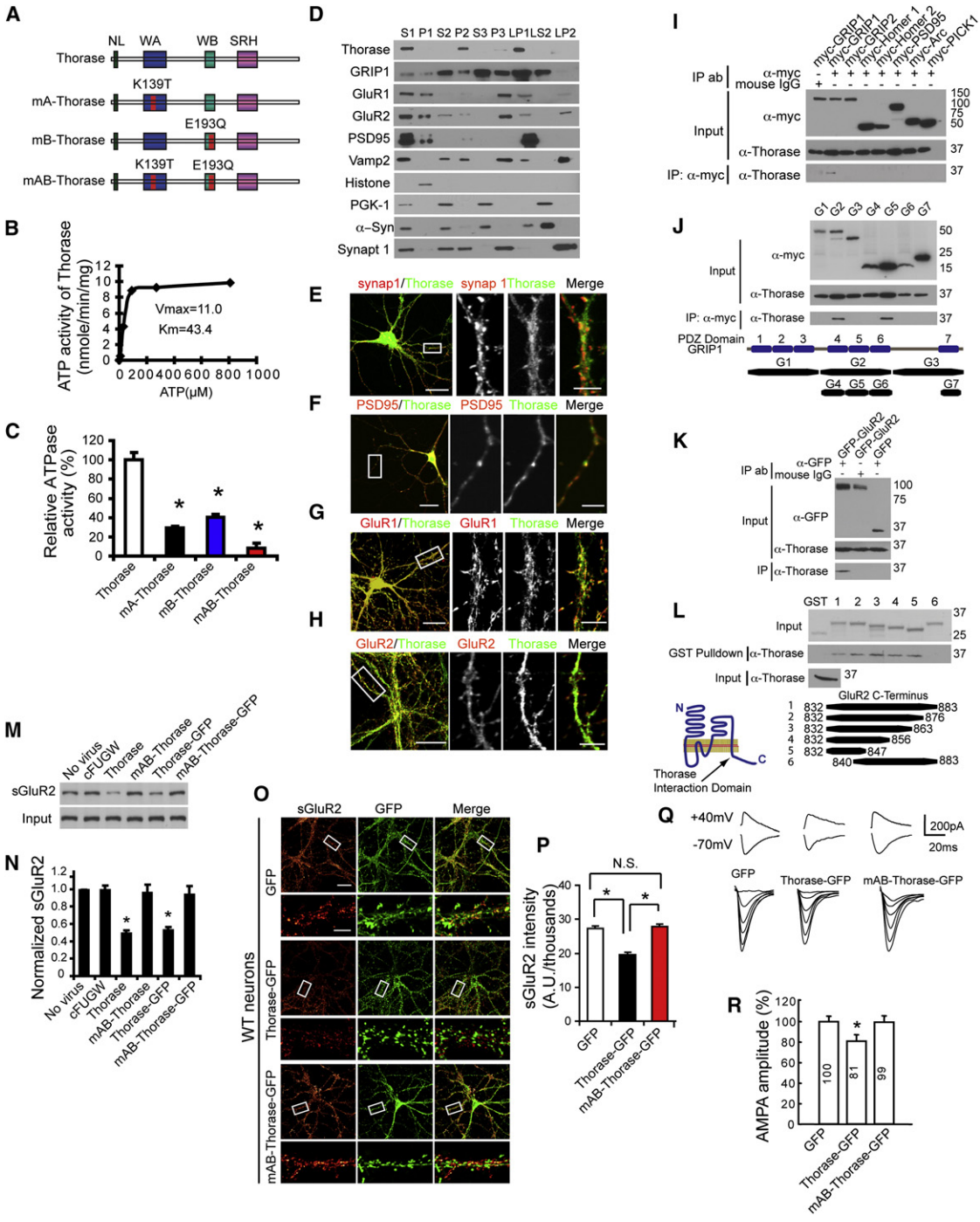

Figure 1. The AAA+ ATPase Thorase Is a Postsynaptic Enriched Protein that Regulates AMPAR Surface Expression

(A) Schematic diagrams of Thorase constructs. WT Thorase (Thorase), Thorase with a Walker A domain mutation (K139T) (mA-Thorase), Thorase with a Walker B domain mutation (E193Q) (mB-Thorase), and Thorase with Walker A and Walker B domains (mAB-Thorase). NL, N-linker; WA, Walker A; WB, Walker B; SRH, second region of homology.

(B) ATPase activity of WT Thorase; V_{max} (nmole/min/mg protein) and K_m (μM).

(C) Analysis of ATPase activities of Thorase mutants (mean ± standard error of the mean [SEM] of three experiments performed in triplicate. n = 3. *p < 0.05, ANOVA with Tukey-Kramer post-hoc test).

(D) Subcellular distribution of Thorase. S1, supernatant of the homogenate at low-speed centrifugation; P1, nuclei and large debris of the corresponding pellet from S1; S2, supernatant of S1 subjected to medium-speed centrifugation; P2, crude synaptosomes of the corresponding pellet from S2; S3, cytosol, which corresponds to the supernatant of S2 subjected to high-speed centrifugation; P3, light membranes, corresponding pellet of S3; LP1, synaptosomal membranes; LS2, synaptic cytosol; LP2, synaptic vesicle-enriched fraction. α-Syn, α-Synuclein; synapt 1, synaptophysin 1.

loss of protein expression in the KO animal (Figures S2D and S2E). Homozygote Thorase KO mice are viable but significantly smaller than their WT littermates (Figure S2F). Approximately 80% of the Thorase KO mice die of a seizure-like syndrome between postnatal days 19 and 25. The remaining 20% survive up to 8 weeks of age (Figure S2G). No gross developmental or behavioral defects are observed between heterozygotes and WT littermates. There are no obvious abnormalities in other tissues in Thorase KO mice at postnatal day 19, as assessed by a comprehensive pathologic necropsy of heart, lung, spleen, kidney, thymus, liver, intestine, testis, eyes, and muscle. Golgi staining of the CA1 region of the hippocampus does not reveal any substantial difference in the dendritic complexity of the Thorase KO mice versus WT mice or in the number or size of dendritic spines (Figures S2H–S2K). Thorase KO mice also show normal density of synapses identified by colocalization of puncta containing both the presynaptic protein synapsin 1 and the postsynaptic protein PSD95 (Figures S2L and S2M). Hematoxylin and eosin (HE) or Nissl staining also show normal brain morphology and intact hippocampi and cortices from Thorase KO mice at P20 (Figures S2N and S2O).

Loss of Thorase Results in an Increase in Surface AMPAR

Levels of AMPAR subunits and associated proteins were assessed in 19- to 23-day-old Thorase KO mice and WT littermates via immunoblot analysis of whole brain lysate and the P2 fraction (Figure 2A). AMPAR subunits GluR1 and GluR2 are increased in both whole brain lysate and the P2 fraction from Thorase KO mice compared to WT littermates (Figure 2A). There is a modest increase in the levels of GRIP1 in whole brain lysate and the P2 fraction in Thorase KO, but there are no obvious differences in PICK1, NMDA receptor 1 (NR1), NR2B, NR2A, PSD95, or synapsin 1 (Figure 2A). In Thorase KO low-density mouse hippocampal neurons, live-cell immuohistochemistry with anti-N-terminal GluR1 or GluR2 antibodies reveals a 23.8% increase in surface GluR1 (Figures 2B and 2C) and a 28.9% increase in surface GluR2 (Figures 2D and 2E). Specificity of these AMPAR increases in Thorase KO neurons is shown by similar expression of surface NR1 between Thorase KO and WT neurons (Figures 2F and 2G). In vivo AMPAR surface expression was assessed by a Bis(sulphosuccinimidyl)suberate (BS^3) crosslinking assay that enables the quantification of surface and intracellular receptor pools. The ratio of surface GluR2/intracellular GluR2 is dramatically increased in the cortex, hippocampus, and cerebellum from Thorase KO mice compared to WT littermates (Figures 2H and 2I). These data suggest that Thorase regulates the distribution of AMPAR and loss of Thorase results in an increase in the steady-state levels of these receptors at the cell surface.

To evaluate the functional outcome of increased AMPAR surface expression, spontaneous miniature excitatory postsynaptic currents (mEPSCs) were assessed in CA1 hippocampal pyramidal neurons from Thorase KO versus WT littermates (Figures 2J–2M). The amplitudes of mEPSCs are increased in Thorase KO compared to WT controls by 70% (Figure 2K), and the frequencies of mEPSCs are similar in neurons from Thorase KO and WT mice (Figure 2L). There is a rightward shift of the cumulative probability distributions of mEPSCs in Thorase KO versus WT neurons, indicating that the increase in amplitude is distributed across the range of recorded events (Figure 2M). The increase in mEPSC amplitude is not due to altered presynaptic activity because paired-pulse facilitation (PPF) was not affected in Thorase KO neurons (see Figure 6B) and no significant difference in the input/output (I/O) curves or amplitude of the field excitatory postsynaptic potentials (fEPSPs) was found in slices from Thorase KO mice compared to WT mice (Figure 6A).

Thorase Regulates Synaptic Scaling

Homeostatic scaling of AMPAR was assessed in WT and Thorase KO low-density hippocampal neurons treated for 48 hr with TTX (1 μM), which blocks all evoked neuronal activity, or bicuculline (20 μM), which increases neuronal firing and blocks inhibitory neurotransmission mediated by $GABA_A$ receptors (Shepherd et al., 2006). WT neurons exhibit a robust increase

(E) Thorase juxtaposes with the presynaptic marker synapsin 1.
(F) Thorase colocalizes, in part, with the postsynaptic marker PSD95.
(G and H) Similar colocalizations with Thorase are also detected for GluR1 and GluR2. Scale bar = 20 μM. High-power images, scale bars = 5 μM.
(I) Thorase interacts with immunoprecipitated (IP) myc-GRIP1, but not other myc-tagged synaptic proteins.
(J) Immunoprecipitated Thorase interacts with the PDZ5 domain of GRIP1. Corresponding protein regions of the fragments are depicted.
(K) Immunoprecipitated Thorase interacts with GFP-GluR2, but not GFP.
(L) GST pull-down assay indicates that Thorase binds to GluR2 residues 832–839 in the C-terminal tail. Coomassie stain of input GST fusion proteins and anti-Thorase immunoblotting of Thorase input are also shown. The illustration depicts the binding region of Thorase on GluR2.
(M) Surface biotinylation assay for GluR2 surface expression in primary high-density cortical cultures infected with different Thorase lentiviruses as indicated. Lenti-cFUGW was used as a lentivirus control.
(N) Quantification of surface levels of GluR2 (mean ± SEM) shown in (M). Student's t test. n = 3. *p < 0.05 when compared with cFUGW.
(O) Representative images of surface GluR2 expression in low-density hippocampal neurons infected with lentivirus expressing GFP, Thorase-GFP, or mAB-Thorase-GFP. Surface GluR2 expression is shown using a Glow scale from black (zero) to red (low pixel intensity) and white (high pixel intensity). Scale bar for low-resolution images = 20 μm. Scale bar for high-resolution images = 5 μm.
(P) Quantification of surface GluR2 expression (mean ± SEM) shown in (O). Student's t test, n = 10–12 cells each group, *p < 0.01, when compared with neurons expressing GFP.
(Q) Representative traces of NMDA and AMPA currents of hippocampal CA1 neurons in slices from mice injected with lenti-GFP, lenti-Thorase-GFP, and lenti-mAB-Thorase-GFP.
(R) Quantification of AMPA amplitudes of hippocampal CA1 neurons in slices from mice injected with lenti-GFP, lenti-Thorase-GFP, and lenti-mAB-Thorase-GFP (mean ± SEM). n = 5 neurons from three different animals for each experimental group, Student's t test, *p < 0.05 when compared with lenti-GFP.
See also Figure S1.

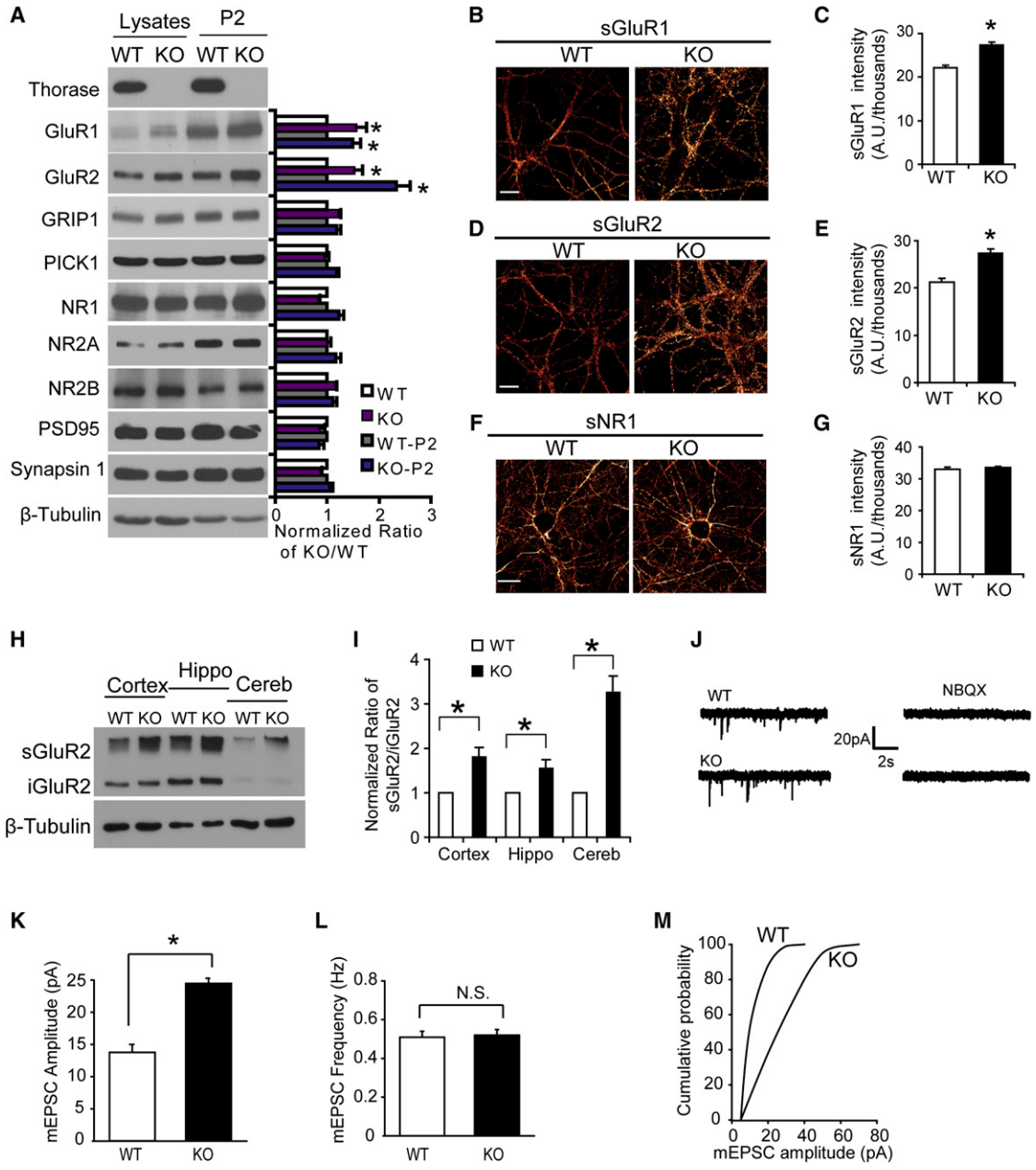

Figure 2. Knockout of Thorase Increases AMPAR Surface Expression and AMPAR Currents

(A) Western blots of synaptic proteins in total brain lysates and P2 fractions obtained from WT and Thorase knockout (KO) mice. Data represent mean ± SEM. Student's t test, n = 3, *p < 0.05, compared with WT mice.

(B) Representative pictures of surface GluR1 in WT and KO primary hippocampal neurons shown using a Glow scale from black (zero) to red (low pixel intensity) and white (high pixel intensity). Scale bar = 20 μm.

(C) Quantification of surface GluR1 levels (mean ± SEM) shown in (B). Student's t test, n = 12–16 neurons each group, *p < 0.05, when compared with WT neurons.

(D) Representative pictures of surface GluR2 in WT and KO primary hippocampal neurons. Scale bar = 20 μm.

(E) Quantification of surface GluR2 levels (mean ± SEM). Student's t test, n = 12–16 cells each group, *p < 0.05, when compared with WT neurons.

(F) Representative pictures of surface NR1 in WT and KO primary hippocampal neurons. Scale bar = 20 μm.

(G) Quantification of surface NR1 levels (mean ± SEM). n = 10–12 neurons each group. Student's t test, p > 0.05, when compared with WT neurons.

(H) BS^3-crosslinking assay to assess surface (sGluR2) and intracellular (iGluR2) GluR2 in WT and Thorase KO brain tissues. Tubulin serves as a loading control between WT and KO. Hippo, hippocampus; Cereb, cerebellum.

(I) Quantification of surface and intracellular GluR2 pools shown in (H) in WT and Thorase KO brain tissues (mean ± SEM, three experiments from three WT and three KO mice, Student's t test, *p < 0.05, when compared with WT neurons).

in surface GluR1 (Figures 3A and 3B) and surface GluR2 (Figures 3C and 3D) with TTX treatment. Bicuculline treatment significantly lowers surface levels of GluR1 (Figures 3A and 3B) and GluR2 (Figures 3C and 3D). In Thorase KO neurons, TTX further increases the surface expression of GluR1 and GluR2 (Figures 3A–3D) but bicuculline has no effect (Figures 3A–3D). These results suggest that in response to activity, AMPAR can be inserted into surface membranes, but removal or endocytosis of AMPAR is blocked in Thorase KO neurons.

Loss of Thorase Results in Reduced Endocytosis of AMPAR

An "antibody feeding" internalization assay for endocytosis of surface GluR2 receptors was performed in live neurons incubated with an anti-GluR2 N-terminal antibody followed by treatment with NMDA (20 μM) and glycine (10 μM) to trigger AMPAR endocytosis (Biou et al., 2008). In WT neurons there is a robust internalization of surface GluR2 but significantly less in Thorase KO neurons (Figure 3E), resulting in a 50% reduction in the internalization index in Thorase KO neurons compared to WT neurons (Figure 3F). These results suggest that Thorase regulates AMPAR scaling by controlling AMPAR endocytosis. No significant difference in internalization of transferrin receptors after stimulation with Alexa 568-conjugated transferrin (Hanley et al., 2002) was detected between Thorase KO and WT neurons (Figures 3G and 3H), indicating that Thorase actions on endocytosis are specific to AMPAR.

AMPAR Trafficking Is ATPase Dependent

pH-sensitive GFP (pHluorin) fused at the N-terminal extracellular domain of GluR1 or GluR2 serves as a spatiotemporal indicator of AMPAR distribution by fluorescing at pH 7.4 at the extracellular surface and becoming nonfluorescent in endosomes where the pH is less than 6.0 (Lin and Huganir, 2007). At baseline, Thorase KO neurons show significantly higher levels of pH-GluR1 and pH-GluR2 signal intensity than WT neurons (Figure S3A). In WT hippocampal cultures, NMDA-stimulated internalization of AMPAR leads to loss of the fluorescent signal for pH-GluR1 or pH-GluR2 (Figures 4A–4E and Figures S3B–S3F), and washout of NMDA leads to recovery of fluorescence consistent with AMPAR endocytosis and recycling as previously described (Lin and Huganir, 2007). In Thorase KO hippocampal cultures, NMDA causes a significantly smaller reduction in fluorescence intensity of both pH-GluR1 and pH-GluR2 and fluorescence recovery is significantly faster than in WT cultures (Figures 4A–4E and Figures S3B–S3F). These results indicate that Thorase is required for AMPAR internalization and that Thorase may inhibit GluR1 and GluR2 recycling back to the plasma membrane.

Rescue experiments were performed in Thorase KO hippocampal cultures with a TdTomato WT Thorase fusion protein with similar ATPase activity to WT Thorase (Figure S3G) and a TdTomato mAB-Thorase fusion protein with an 80% reduction of ATPase activity (Figure S3G) in the presence of either the pH-GluR1 or pH-GluR2 in Thorase KO cultures (Figures 4F–4I and Figures S3G and S3H). NMDA-stimulated AMPAR trafficking in Thorase KO cultures is restored to WT levels by WT Thorase, whereas the mAB-Thorase fails to alter AMPAR trafficking deficits in Thorase KO cultures (Figures 4F–4I and Figure S3H). These results taken together indicate that NMDA-stimulated AMPAR internalization is mediated by Thorase in an ATPase-dependent manner and that inhibition of GluR1 and GluR2 recycling back to the plasma membrane by Thorase is ATPase dependent.

Thorase Provides a Driving Force to Disassemble the AMPAR Complex

AAA^+ ATPases often assist in the assembly or disassembly of protein complexes (Ogura and Wilkinson, 2001; White and Lauring, 2007). To explore whether Thorase may function as an energy motor that dissociates the AMPAR complex to facilitate endocytosis, AMPAR complexes were prepared from brains of WT and Thorase KO mice in the presence or absence of ATP or nonhydrolyzable ATPγS (Figure 5A). Immunobloting with anti-GluR2 antibody shows that AMPAR complexes were well prepared and migrate at approximately 700 kDa. In the presence of ATP, a substantial portion of the AMPAR complex from WT mouse brains shifts to approximately 300 kDa (Figure 5A). However, in the presence of ATPγS, the position of the AMPAR complex remains stable. In contrast, AMPAR complexes from Thorase KO mouse brains show no difference in the presence or absence of ATP or ATPγS (Figure 5A). Coimmunoprecipitation from mouse hippocampal extracts with an anti-GluR2 antibody shows that GluR2, GRIP1, and Thorase coexist as a complex in vivo (Figure 5B). The binding of GRIP1 and Thorase to the GluR2 complex is sensitive to ATP hydrolysis as there is more binding in the presence of ATPγS and less binding in the presence of ATP (Figures 5B and 5C). These results taken together support the notion that the ATPase activity of Thorase is required for the disassembly of native AMPAR complexes in vivo.

To confirm whether Thorase directly interacts with GluR2 and GRIP1, GST-GluR2 C terminus (R2C) and GST-GRIP1 were expressed and immobilized on the glutathione agarose beads, respectively. Thorase binds GluR2C in the presence of nonhydrolyzable Mg^{2+}/ATPγS or EDTA/ATP (Figure 5D). In the presence of hydrolyzable ATP, Thorase is not retained by GST-GluR2C (Figure 5D). Thorase weakly binds GRIP1 in the presence of ATPγS (Figure 5E). However, when GluR2C is

(J) Representative mEPSC recordings in CA1 hippocampal neurons in brain slices from WT and KO mice (postnatal days 19–21). Recordings were made for 10 s in neurons held at −70 mV in the presence of 50 μM TTX and 100 μM Picrotoxin. 2060 events from WT mice (4 mice, 16 slices, and 22 neurons) and 1816 events from KO mice (3 mice, 12 slices, and 20 neurons) were recorded.

(K) Average mEPSC amplitudes are significantly increased in KO hippocampal neurons compared with WT neurons (mean ± SEM). Student's t test, *$p < 0.05$.

(L) The mEPSC frequency is not significantly increased in KO hippocampal neurons compared with WT neurons (mean ± SEM). Student's t test, $p > 0.05$.

(M) Cumulative probability distributions of mEPSC amplitudes for WT and KO neurons show scaled-up amplitudes in KO neurons.

See also Figure S2.

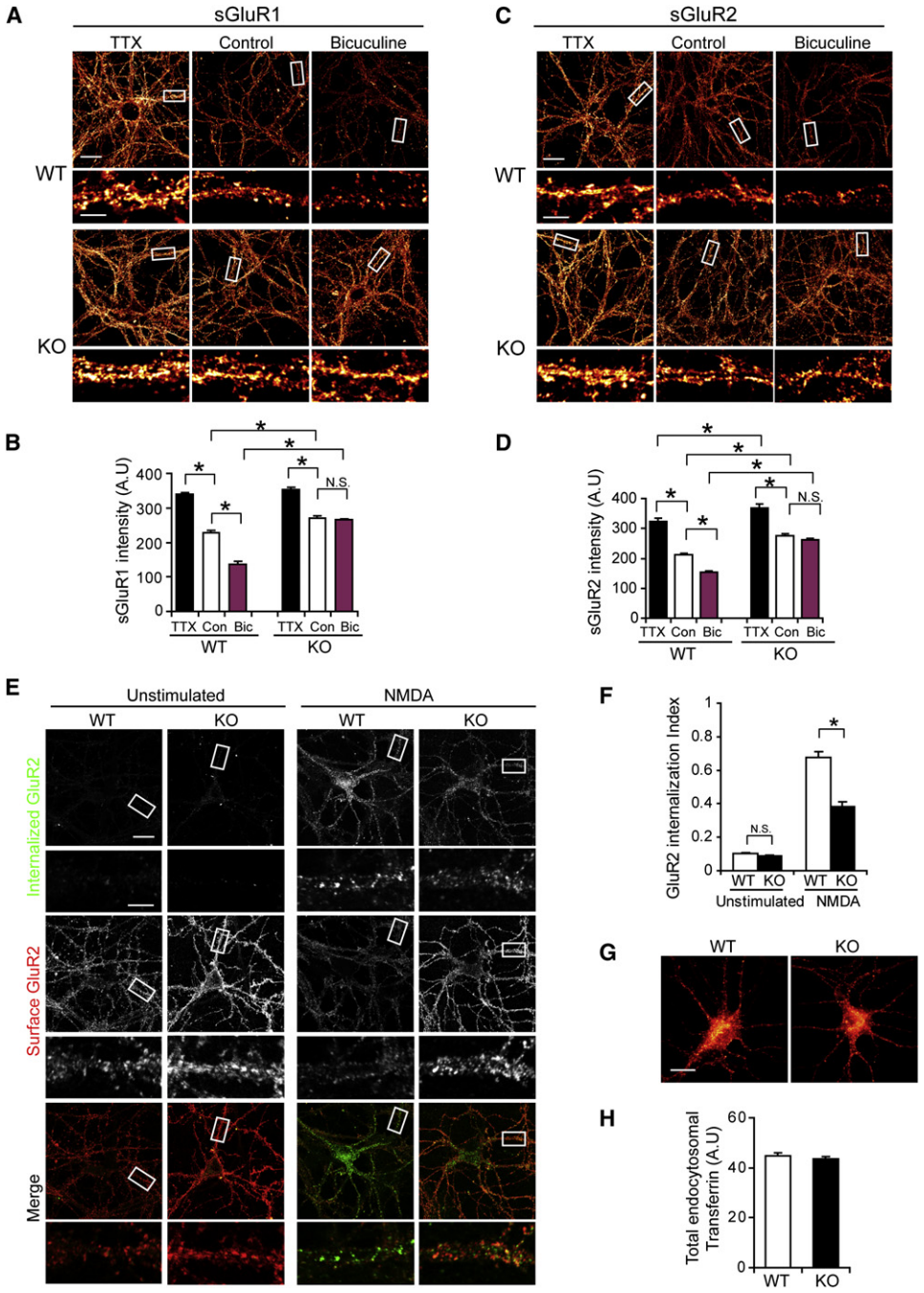

Figure 3. Deficits in Homeostatic Synaptic Scaling and Endocytosis of AMPAR in Thorase KO Neurons

(A) Representative images of surface GluR1 in hippocampal WT and KO neurons treated with TTX (1 μM) or bicuculline (20 μM) for 48 hr. No treatment was used as control. Surface AMPAR expression is shown using a Glow scale from black (zero) to red (low pixel intensity) and white (high pixel intensity). Low-resolution image scale bar = 20 μm. High-resolution image scale bar = 5 μm.

(B) Quantification analysis of surface levels of GluR1 in WT and KO neurons in (A) after TTX or bicuculline treatment (mean ± SEM). Two-way ANOVA, n = 10–16 cells each group,*$p < 0.05$.

(C) Representative images of surface GluR2 in hippocampal WT and KO neurons treated for 48 hr with TTX (1 μM) or bicuculline (20 μM). No treatment was used as control. Surface GluR2 expression is shown using a Glow scale from black (zero) to red (low pixel intensity) and white (high pixel intensity). Scale bar = 20 μm; High-resolution image scale bar = 5 μm.

(D) Quantification analysis of surface GluR2 intensities in WT and KO neurons after TTX and bicuculline treatment (mean ± SEM). Two-way ANOVA, n = 10–16 cells each group, *$p < 0.01$.

(E) Representative images of NMDA-induced endocytosis of AMPAR in WT or KO neurons. Robust internalization of GluR2 was induced in WT neurons by NMDA treatment (20 μM, 5 min), whereas KO neurons show less internalization. Scale bar = 20 μm; High-resolution image scale bar = 5 μm.

preincubated with GRIP1 to form GluR2C-GRIP1 complexes, Thorase shows robust binding to GluR2C-GRIP1 complexes in the presence of ATPγS (Figure 5F), indicating that Thorase prefers to bind to AMPAR complexes containing GRIP1. However, in the presence of ATP, Thorase binding to GluR2C-GRIP1 complexes is disrupted, suggesting that this binding is sensitive to ATP hydrolysis (Figure 5F).

To test whether, in the presence of ATP, Thorase might disrupt GluR2-GRIP1 interactions, His_6-GRIP1 protein was immobilized on Dynabeads, incubated with GST-GluR2C to form His_6-GRIP1/GST-GluR2C complexes, and then incubated with GST-Thorase in the presence of ATP or ATPγS (Figure 5G). In the presence of ATPγS, the complex of His_6-GRIP1/GST-GluR2C is stable (Figure 5Gb), but in the presence of ATP there is a striking dissociation of GST-GluR2C from His_6-GRIP1 (Figure 5Gb). Additionally, in the presence of ATPγS, the His_6-GRIP1/GST-GluR2C complexes are stable even at high concentration of GST-Thorase. In contrast, in the presence of ATP, 200 nM of GST-Thorase causes 75% disassembly of His_6-GRIP1/GST-GluR2C complexes, with nearly complete disassembly in the presence of 400 nM of GST-Thorase (Figure 5H). Taken together, these results indicate that dissociation of GRIP1 and AMPAR complexes requires Thorase ATPase activity.

Loss of Thorase Blocks LTD at Schaffer Collateral Synapses

To determine whether Thorase plays a role in regulating synaptic plasticity, postsynaptic responses of CA1 neurons were recorded during and after stimulation of presynaptic Shaffer collateral axons in hippocampal slices from WT and Thorase KO mice. There are no significant differences in the input/output (I/O) curves or amplitudes of fEPSPs or paired-pulse facilitation (PPF) in slices from Thorase KO mice compared to WT mice (Figures 6A and 6B). Collectively, these findings suggest that Thorase does not play a major role in basal transmission at CA1 synapses.

LTD and LTP were evaluated in Thorase KO and WT mice. LTD was induced in slices from WT littermates with persistent depression of evoked response (74.9% ± 12.1% of the baseline), whereas LTD was absent in slices from Thorase KO mice (105.7% ± 14.3% of the baseline) (Figure 6C). LTP was induced in slices from WT and Thorase KO mice with the magnitude of LTP greater in slices from Thorase KO mice (204.2% ± 28.6%) compared to WT mice (169.9% ± 27.7%) (Figure 6D). These changes were not due to alterations in gross anatomy (Figures S2N and S2O) or normal basal synaptic transmission.

NMDA and AMPA currents were recorded simultaneously by whole-cell patch-clamp during a series of voltage steps. The NMDA receptor antagonist D-AP5 blocks the current induced at a positive potential (Figure 6E). The AMPAR antagonist, CNQX, abolishes currents at all stimulation voltages; this effect is reversed during a 20–30 min washout period (Figure 6E). The maximum amplitude of the AMPA current is significantly greater in slices from the Thorase KO mice compared to the WT mice at all stimulus voltages tested (Figure 6F). No significant change was found in the amplitude of NMDA currents. The ratio of AMPA current/NMDA current was increased about 30% (Figure 6F). There is a significant rightward shift in the current-voltage (I-V) curve at negative stimulation potentials in slices from Thorase KO mice compared to WT mice (Figure 6G). There is still a significant rightward shift in the I-V curve at negative stimulation potentials in the presence of the NMDA inhibitor D-AP5 in Thorase KO slices, confirming that the increased AMPA current is caused by increased surface AMPAR (Figure 6H).

The AMPAR rectification index was measured by dividing the excitatory postsynaptic current (EPSC) amplitude at +40 mV by that at −70 mV (Isaac et al., 2007). There is no significant difference in the rectification index between WT and Thorase KO mice (Figure 6I), suggesting that there is no alteration in the synaptic AMPAR composition in Thorase KO mice. Philanthotoxin 433 (PhTx), a specific antagonist of the GluR2-lacking AMPAR, did not alter the I-V curves in neurons from WT and KO mice (Figures S4A–S4C), suggesting that GluR2-containing AMPAR predominated in both WT and KO neurons. Although the surface levels of GluR1 and GluR2 in KO neurons are higher than those of WT neurons evaluated by immunohistochemistry, there is no significant change in the ratio of surface GluR2 to GluR1 between WT and KO neurons (Figures S4D and S4E). These results taken together indicate that knockout of Thorase does not affect AMPAR subunit composition.

Thorase was reintroduced into Thorase KO hippocampus by stereotaxic injection of lenti-GFP, lenti-Thorase-GFP, and lenti-mAB-Thorase-GFP virus. One week later, hippocampal slices were generated for physiology. There is no effect on AMPAR currents from lenti-GFP (Figures 6J and 6K); however Thorase-GFP restores AMPAR currents back to WT levels, whereas, mAB-Thorase-GFP has no rescue effect (Figures 6J and 6K). In hippocampal culture, the increased surface expression of GluR2 in Thorase KO neurons could also be rescued by lentiviral expression of Thorase-GFP but not by mAB-Thorase-GFP or GFP (Figures S4F and S4G). Taken together, these results indicate that the increase in AMPA current in Thorase KO mice results from lack of Thorase and not a nonspecific process due to the absence of Thorase, and the functional effects are ATPase dependent.

Thorase Is Essential for Learning and Memory

To avoid the lethality of Thorase KO mice, *Thorase*$^{flox/+}$ mice were crossed with CaMKIIa-iCre transgenic mice to restrict the temporal and spatial deletion of Thorase to the adult forebrain. Immunoblot analysis and immunohistochemistry verify that

(F) Quantification of internalization index shown in (E) as measured as the ratio of integrated fluorescence intensity of internalized GluR2 to the total fluorescence intensity (integrated fluorescence intensity of internalized GluR2 plus surface GluR2). Data represent mean ± SEM (n = 6–11 neurons for each condition. Student's t test, *p < 0.001).

(G) Thorase KO hippocampal neurons show normal transferrin receptor endocytosis induced by stimulation with Alexa 568-conjugated transferrin for 15 min at 37°C. Scale bar = 20 μm.

(H) Quantitation of internalized transferrin receptors in neurons shown in (G). Values represent total internalized Alexa 568-conjugated transferrin (mean ± SEM, n = 10, Student's t test, p > 0.05).

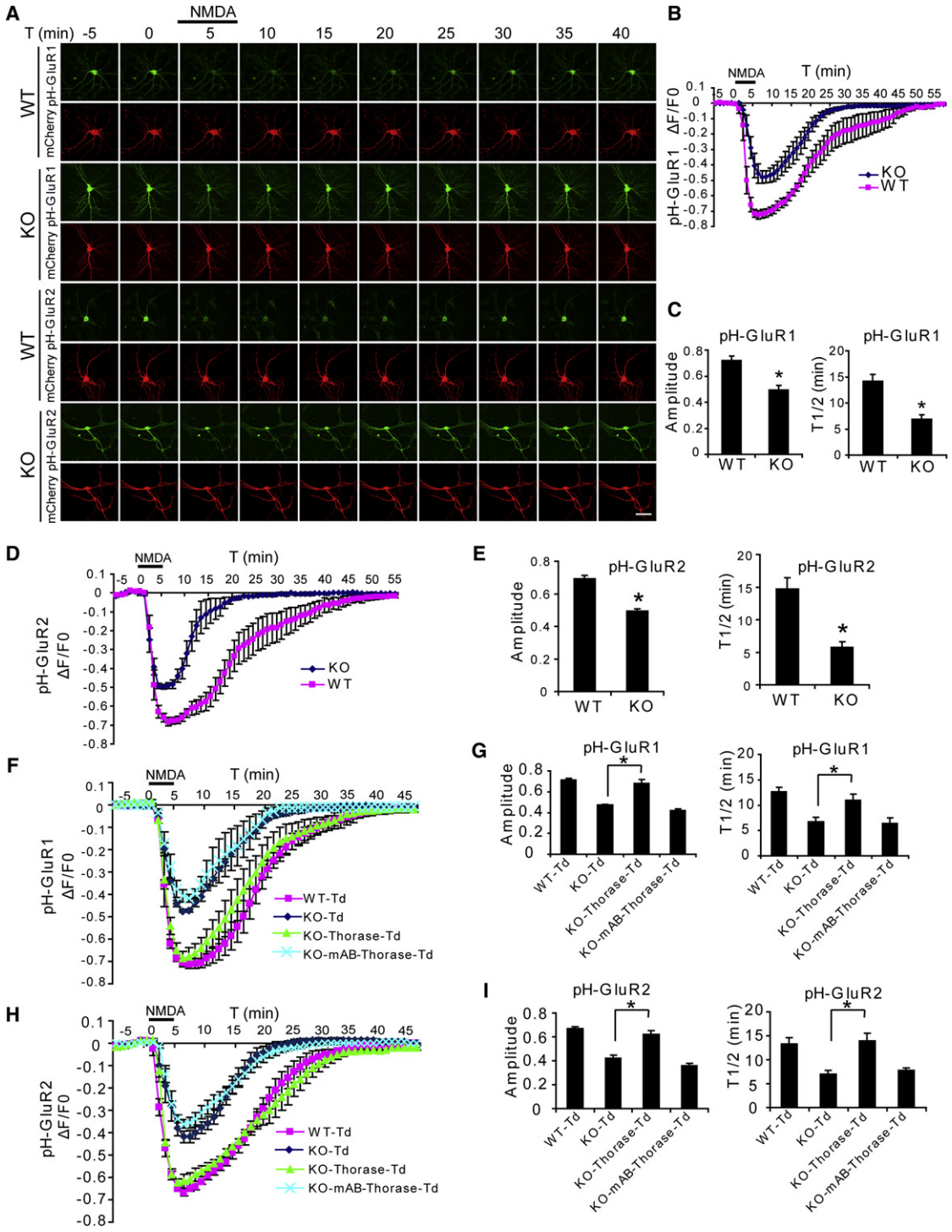

Figure 4. NMDA-Induced AMPAR Internalization Is Reduced in an ATPase-Dependent Manner in Thorase KO Neurons

(A) Representative images of hippocampal neurons transfected with pHluorin (pH)-GluR1 or pH-GluR2 and mCherry subjected to a NMDA (20 μM, 5 min)/washout cycle. Scale bar = 50 μm.

(B) Time trace of pH-GluR1 fluorescence change in response to NMDA perfusion for the experiment presented in (A) (mean ± SEM, n = 6 neurons for each experimental group from three individual experiments).

(C) Maximum amplitudes of pH-GluR1 fluorescence intensity changes to NMDA stimulation and average recycling half-time ($T_{1/2}$, the time taken from maximum endocytosis to 50% recycling) after NMDA washout (mean ± SEM, n = 6 neurons from three experiments. *p < 0.01, compared with WT neurons, Student's t test).

(D) Time trace of pH-GluR2 fluorescence change in response to NMDA perfusion for the experiment presented in (A).

Thorase is largely eliminated from forebrain structures including the hippocampus and cortex but not in other regions such as the cerebellum (Figure S5). There are no gross anatomical changes in the hippocampus or other forebrain structures in the conditional Thorase KO (cKO) mice compared to WT control (Figure S5).

The general activity of Thorase cKO mice was assessed in open field testing (Pletnikov et al., 2008) in which Thorase cKO mice spend more time at the margins of the open field and less time in the center and show less rearing activity (Figures 7A–7C). This is not due to altered anxiety as there was no significant difference in performance on the elevated plus maze (Walf and Frye, 2007) in the total distance, percent open time, percent entrance to open arms, or the number of rearing behaviors (Figures 7D–7G). These results suggest that the deficits in the open field could be due to the inability to form immediate memories in a novel environment. Assessment of spatial memory using the Morris Water Maze test was not possible due to seizures in the conditional Thorase KO mice. Accordingly, spatial memory was determined in spontaneous alteration in a Y-maze using a continuous trials procedure. The Thorase cKO mice have a lower percentage of correct alternating arm entries compared to the littermate WT mice (Figure 7H), indicating that the Thorase cKO mice are amnesic when reintroduced into a previously novel environment. Seven days after exposure to the Y-maze, mice were placed for 5 min into a Y-maze in which the third arm was closed to acquire contextual memory (Etkin et al., 2006). Whereas the WT mice spent more time in the novel arm that was previously blocked, the Thorase cKO mice spent significantly less time in the novel arm (Figure 7I), suggesting deficits in short-term memory. To exclude the possibility for a Y-maze side preference, a T-maze nonmatching-to-place task was performed to test hippocampal-dependent spatial working memory (Deacon and Rawlins, 2006; Reisel et al., 2002). WT mice show a strong nonmatching-to-place performance for a sweet milk reward, attaining a 90% correct choice by the end of training (Figure 7J). In contrast, the Thorase cKO mice are impaired and remain at chance levels at the end of training (Figure 7J) (58%, $F_{1,\ 44} = 15.1$, $p < 0.002$). These behavioral data indicate that the knockout of Thorase has profound effects on learning and memory, consistent with the effects of Thorase on AMPAR function.

DISCUSSION

The major finding of this paper is that the AAA$^+$ ATPase Thorase is a significant and important regulator of AMPAR trafficking, synaptic plasticity, and behavior. A major mechanism regulating synaptic strength is the net balance between the insertion and internalization of AMPAR in the postsynaptic membrane (Kerchner and Nicoll, 2008; Sudhof and Malenka, 2008). Our data show that surface levels of AMPAR in Thorase KO neurons are increased with chronic TTX treatment, whereas bicuculline treatment fails to lower the surface levels of AMPAR in Thorase KO neurons, indicating that the process of AMPAR insertion is intact and that internalization is impaired. This is also strongly supported by the impaired NMDA-stimulated internalization of GluR2 receptors as detected by the "antibody feeding" assay. Moreover, the spatiotemporal indicators of AMPAR distribution, pH-GluR1 or pH-GluR2, indicate that Thorase is involved in AMPAR internalization and that Thorase may inhibit GluR1 and GluR2 recycling back to the plasma membrane in an ATPase-dependent manner. In addition, the impaired LTD in Thorase KO neurons occurs immediately during the 1 Hz stimulation protocol, indicating that the absence of LTD is due to a deficit in the mechanism of LTD induction. Because LTD in hippocampal CA1 neurons is mainly initiated postsynaptically by the removal of surface AMPAR through endocytosis (Kessels and Malinow, 2009; Massey and Bashir, 2007), these findings taken together suggest that Thorase is involved in the process of AMPAR endocytosis and that the lack of Thorase causes impaired internalization of AMPAR.

Thorase belongs to an AAA$^+$ ATPase family that often performs chaperone-like functions, including membrane dynamics, protein transport, and assembly or disassembly of protein complexes without unfolding or destroying their target proteins (Ogura and Wilkinson, 2001; White and Lauring, 2007). Numerous ATPases are expressed in neurons that regulate many key cellular functions. In this study, two-dimensional gel separations show that the ATPase activity of Thorase is required for the disassembly of AMPAR complexes in vivo, suggesting that Thorase plays a crucial role in disassembly of the AMPAR complex. Endogenous coimmunoprecipitation assays show that GluR2, GRIP1, and Thorase coexist as a complex in vivo and the binding of Thorase to GluR2 is sensitive to ATP hydrolysis. In vitro binding experiments further confirmed that Thorase can directly bind to GluR2 and GRIP1 and that this binding is highly sensitive to ATP hydrolysis. Intriguingly, Thorase prefers to bind the GluR2-GRIP1 complex in the presence of nonhydrolyzable ATPγS, and Thorase robustly disassembles GluR2-GRIP1 complexes in the presence of ATP, indicating that Thorase may mainly function on surface AMPAR complexes. GRIP1 acts as an AMPAR anchor stabilizing AMPAR at the plasma membrane and limits the endocytosis rate of AMPAR

(E) Maximum amplitudes of pH-GluR2 fluorescence changes to NMDA and $T_{1/2}$ after NMDA washout (mean ± SEM, n = 6 neurons from three experiments. *$p < 0.01$, compared with WT neurons, Student's t test).
(F) Fluorescence changes for pH-GluR1 in hippocampal WT and KO neurons transfected with tdTomato (Td), Thorase-Td, or mAB-Thorase-Td during NMDA perfusion/washout experiments (mean ± SEM, n = 5 neurons from three experiments).
(G) Maximum amplitudes of pH-GluR1 fluorescence changes to NMDA and $T_{1/2}$ after NMDA washout (mean ± SEM, n = 5 neurons from three experiments. *$p < 0.01$, two-way ANOVA with Tukey-Kramer post-hoc test).
(H) Fluorescence changes for pH-GluR2 in hippocampal WT and KO neurons transfected with Td, Thorase-Td, or mAB-Thorase-Td during NMDA perfusion/washout experiments (mean ± SEM, n = 5 neurons from three experiments).
(I) Maximum amplitudes of pH-GluR2 fluorescence changes to NMDA and $T_{1/2}$ after NMDA washout (means ± SEM, n = 5 neurons from three experiments. *$p < 0.01$, two-way ANOVA with Tukey-Kramer post-hoc test).
See also Figure S3.

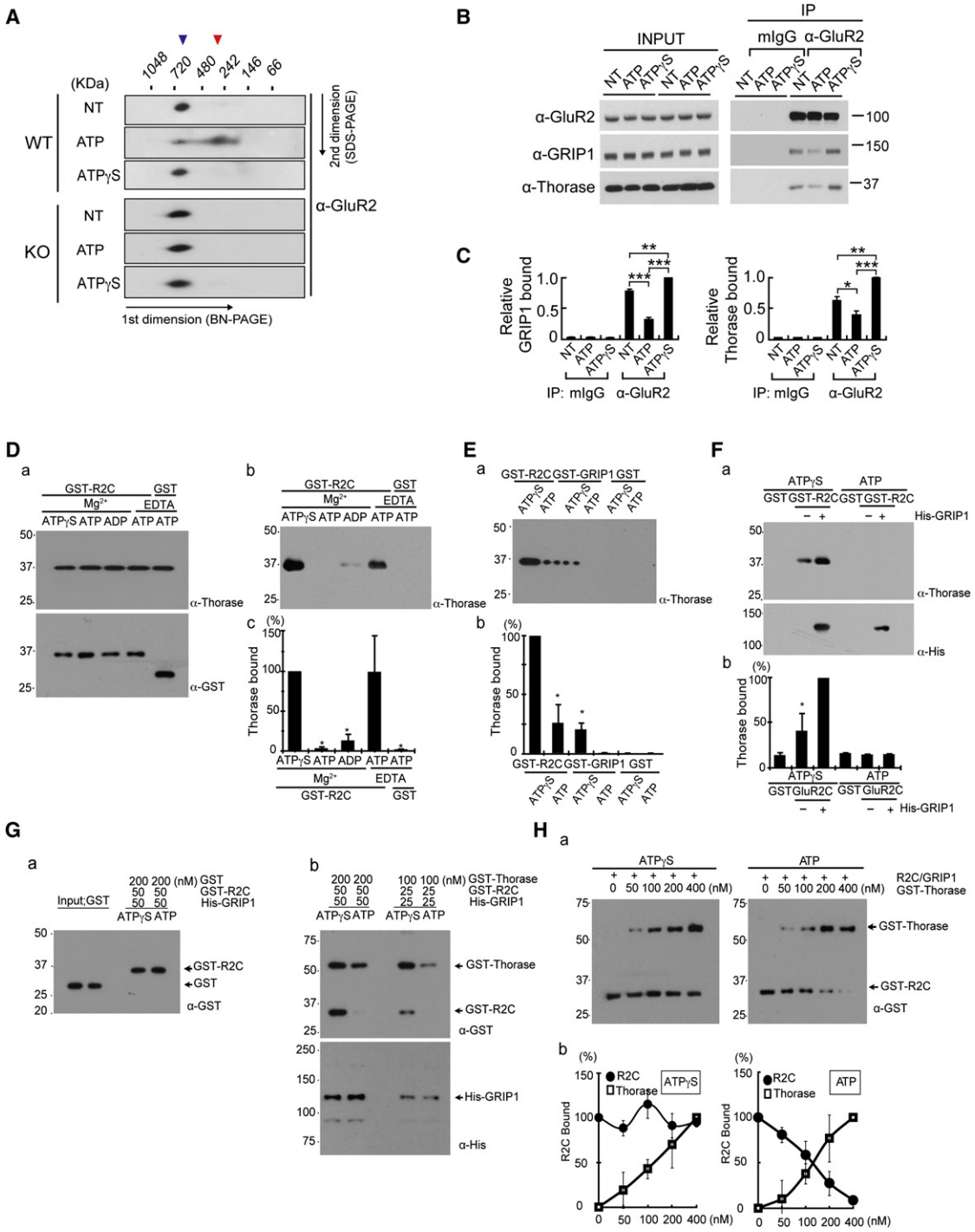

Figure 5. Thorase Provides a Driving Force to Disassemble the AMPAR Complex

(A) Thorase WT or KO hippocampal homogenates solubilized in NativePAGE sample buffer containing either 1 mM ATP or ATPγS were separated by blue-native two-dimensional PAGE (BN-2DE-PAGE) and immunoblotted with anti-GluR2 antibody. Blue arrowhead demarcates AMPAR complex and red arrowhead indicates disrupted AMPAR complex. Repeated with similar results, n = 3.

(B) Thorase, GluR2, and GRIP1 form an ATP-dependent complex in mouse hippocampus. Hippocampal homogenates were immunoprecipitated with anti-GluR2 with 1 mM ATP or ATPγS. Protein interaction was analyzed by immunoblot using anti-GRIP1 or anti-Thorase antibodies.

(C) Binding data from (B) were quantitated by scanning densitometry. Values are relative to the ATPγS condition (mean ± SEM, n = 4, *p < 0.05, **p < 0.01, ***p < 0.001, Student's t test).

(D) ATP-dependent interaction between Thorase and a GST fusion protein containing the C terminus (amino acids 832–883) of GluR2 (GST-R2C). One hundred nanomoles GST-R2C or GST alone was immobilized on glutathione agarose beads and then 200 nM Thorase was applied to the beads in Buffer A containing

by its association with GluR2 (Dong et al., 1997; Osten et al., 2000; Shepherd and Huganir, 2007). Therefore, we propose a mechanism in which GluR2, GRIP1, and Thorase form a complex in the presence of ATP and Thorase provides the ATP-driving force to disrupt GluR2-GRIP1 interactions, resulting in dissociation of the AMPAR complex. Thorase-mediated disassembly of AMPAR complexes appears to play a crucial role in limiting endocytosis of AMPAR to adjust the level of AMPAR at the synaptic membrane. The regulation of disassembly of AMPAR by Thorase is likely to account for its essential roles in LTD and regulation of synaptic plasticity and learning memory because LTD is at least partly expressed by removal of AMPAR from the synapse by endocytosis (Turrigiano, 2000).

The related AAA^+ ATPase NSF is another postsynaptic protein that is required for disassembly of the SNARE complex (Ungermann et al., 1998) and for AMPAR trafficking (Nishimune et al., 1998). NSF binds to the AMPAR subunit GluR2 and disassembles the GluR2-PICK1 protein complex and regulates excitatory synaptic plasticity by stabilizing or recycling AMPAR into postsynaptic membranes (Hanley et al., 2002). In contrast, Thorase acts at GluR2-GRIP1 complexes to control the endocytosis and removal of AMPAR from the postsynaptic membrane. The identification of Thorase as a major regulator of AMPAR trafficking offers new opportunities to enhance the understanding and to identify additional regulators of AMPAR turnover.

EXPERIMENTAL PROCEDURES

Antibodies

Monoclonal and polyclonal Thorase antibodies were generated as described in Extended Experimetnal Procedures. GluR1-N (mAb) was a gift from Dr. Richard L. Huganir. Other antibodies were acquired commercially: GluR2-N (mAb, Chemicon) and GluR2 (pAb, Millipore), PSD95 (mAb, NeuroMab), synaptophysin 1 (mAb, Sigma), synapsin 1 (pAb, mAb, BD Tranduction Laboratories), PICK1 (mAB, NeuroMab), NR1 (pAb, Sigma), NR2A (mAb, Sigma), NR-2B (mAb, NeuroMab), β-tubulin (mAb, Sigma), and GRIP1 (pAb, Chemicon).

ATPase Activity Assay

The ATPase activities of Thorase and its mutants were determined by the measurement of the amount of [γ-^{32}P]-Pi obtained from [γ-^{32}P]-ATP hydrolysis using EasyRad Phosphate Assay Biochem Kit (Cytoskeleton Inc, Denver, CO, USA) according to the instruction from the manufacturer (Extended Experimetnal Procedures).

Primary Neuronal Cultures and Transduction of Cultured Neurons with Recombinant Lentivirus

Primary cortical neuron cultures were prepared from embryonic day 15 (E15) mouse pups as described (Shepherd et al., 2006). Low-density hippocampal neurons from E18 or postnatal day 0–1 mouse pups were prepared as reported previously (Shepherd et al., 2006). Neurons were infected with different lentivirus 10 days after plating.

Electrophysiology

Thorase KO and WT littermates with the age of postnatal days 19–22 were used for all electrophysiological experiments. Transverse hippocampal slices (350 μm) were prepared and maintained recordings were performed as described in our previous studies (Wang et al., 2004) (Extended Experimetnal Procedures). Excitatory postsynaptic currents (EPSCs) were recorded from CA1 pyramidal neurons (Wang et al., 2009) (Extended Experimetnal Procedures).

Behavioral Experiments

All behavioral experiments were done in 3- to 4-month-old cKO (*Thorase*$^{Flox/Flox,\ cre+}$) mice (n = 20, 10 males and 10 females) and WT (*Thorase*$^{+/+,\ cre+}$) littermates (n = 19, 9 males and 10 females), which were obtained by mating heterozygous *Thorase*$^{Flox/+,\ cre+}$ mice. Both the sex and the age were matched between two groups.

Open Field

Open field test was performed to assess the general activity of Thorase KO mice using Photobeam Activity System (San Diego Instruments Inc., La Jolla, CA, USA), which records both horizontal and vertical activities simultaneously (Extended Experimetnal Procedures).

Elevated Plus Maze

Anxiety-like behavior was evaluated in Elevated Plus Maze (San Diego Instruments Inc.) as described previously (Singer et al., 2009) (Extended Experimetnal Procedures).

Y-Maze

Spontaneous alternation was assessed by Y-maze test using a protocol similar to those previously described (Holcomb et al., 1998; Hsiao et al., 1996) (Extended Experimetnal Procedures).

Mg^{2+} or EDTA plus ATP or ATPγS as indicated. (a) Input proteins were analyzed by immunoblotting with anti-Thorase and anti-GST-HRP antibodies. (b) Bound Thorase was detected by immunoblotting using anti-Thorase antibody. (c) Quantification of immunoblots in (b). Values are relative to Mg^{2+}/ATPγS (mean ± SEM, n = 3, *p < 0.05 by ANOVA with Tukey-Kramer's post-hoc test).

(E) Thorase strongly binds to GST-R2C rather than GST-GRIP1. Fifty nanomoles of GST-R2C, GST-GRIP1, or GST alone was immobilized on glutathione agarose beads and then incubated with 200 nM Thorase in Buffer B plus ATP or ATPγS as indicated. (a) Bound Thorase was detected by immunoblotting using anti-Thorase antibody. (b) Quantification of immunoblots in (a); values are relative to ATPγS in the first lane (mean ± SEM; n = 3, *p < 0.05 by ANOVA with Tukey-Kramer's post-hoc test).

(F) Thorase binds to GST-R2C/GRIP1 complex more strongly than GST-R2C alone. Fifty nanomoles of GST-R2C immobilized on glutathione agarose beads in presence or absence of His_6-GRIP1 (50 nM), followed by incubation with 200 nM Thorase plus ATP or ATPγS. (a) Bound Thorase or His-GRIP1 was detected by immunoblotting using anti-Thorase and anti-His antibodies. (b) Quantification of immunoblots in (a); values are relative to GST-R2C/GRIP1 condition in the third lane (mean ± SEM, n = 3, *p < 0.05 by ANOVA with Tukey-Kramer's post-hoc test).

(G) Thorase disrupts the GST-R2C/GRIP1 complex in an ATP-dependent manner. Either 50 nM or 25 nM of His_6-GRIP1 was immobilized on Dynabeads for His-tag Isolation and then GST-R2C was sequentially applied as indicated. (a) Two hundred nanomoles of GST was incubated with the His_6-GRIP1/GST-R2C complex plus ATP or ATPγS as indicated. GST alone was not detected by immunoblotting using an anti-GST antibody. (b) GST-Thorase was incubated with the His_6-GRIP1/GST-R2C complex in buffer B plus ATP or ATPγS as indicated. Bound GST-Thorase was detected by immunoblotting using anti-GST antibody.

(H) Dose-response curve for Thorase dissociation of GRIP1/GST-R2C complexes. (a)The same assay as in (G) was carried out with different concentrations of GST-Thorase (nM) as indicated. A plus sign (+) denotes the addition of the His_6-GRP1 (50 nM)/GST-R2C (50 nM) complex. (b) Dose-response curve for Thorase disassembling GRIP1/GST-R2C complexes shows data of quantification of immunoblots from three experiments in (a) (mean ± SEM, n = 3), values are relative to zero [Thorase] condition.

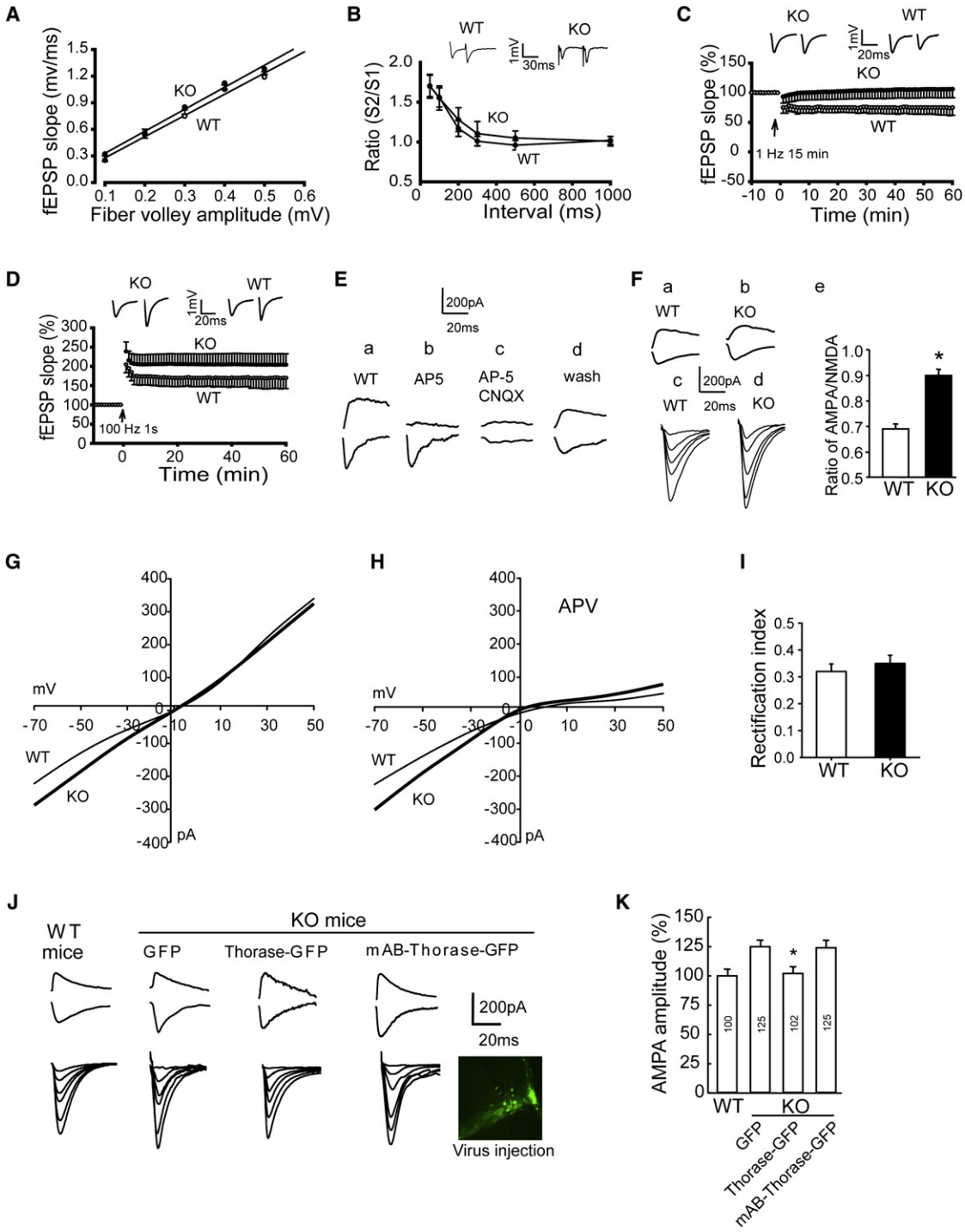

Figure 6. Thorase Deficiency Enhances AMPAR Currents and LTP and Impairs LTD without Affecting Basal Synaptic Transmission at CA1 Hippocampal Synapses

(A) Thorase KO CA1 neurons exhibit normal basal synaptic transmission. The amplitude of the fiber volley is plotted against fEPSP slopes. The input/output curves for neurons in slices from WT (n = 8 slices, 8 mice) or KO (n = 6 slices, 6 mice) were not significantly different (mean ± SEM, $p > 0.05$, Student's t test).

(B) Thorase KO does not affect paired-pulse facilitation (PPF) (WT, n = 8 slices, 6 mice; KO, n = 12 slices, 8 mice) (mean ± SEM, $p > 0.05$, Student's t test).

(C) Thorase is necessary for LTD induction. LTD was induced by stimulation (1 Hz, 15 min) in slices from WT mice but not in slices from Thorase KO mice (mean ± SEM, KO, n = 8 slices from five mice; WT, n = 6 slices from four mice).

(D) Thorase is a negative regulator of LTP. LTP was induced by a tetanic train (100 Hz, 1 s). The magnitude of LTP for slices from KO mice was significantly greater than that for WT mice (mean ± SEM, KO, n = 8 slices from 4 mice; WT, n = 6 slices from three mice. $p < 0.01$, Student's t test).

T-Maze

To avoid side preferences of some animals in Y-maze test, spatial nonmatching-to-place testing was performed on an elevated T-maze according to the protocol previously described (Deacon and Rawlins, 2006; Reisel et al., 2002) (Extended Experimetnal Procedures).

Statistics

Quantitative data are presented as the mean ± standard error of the mean (SEM). Statistical significance was either assessed via an unpaired two-tailed Student's t test or an ANOVA test with Tukey-Kramer post-hoc analysis. All behavioral data were first subjected to a Kolmogorov-Smirnov normality and an equal variance test. For open field and T-maze test, repeated-measures two-way ANOVAs were conducted and significant differences were determined at $p < 0.05$ for group main effects. The points with significant differences were identified by post-hoc analysis using the Holm-Sidak method for multiple comparisons. For elevated plus maze and Y-maze tests, all data were analyzed using a Student's t test. Assessments were considered significant with a $p < 0.05$.

SUPPLEMENTAL INFORMATION

Supplemental information includes Extended Experimental Procedures and five figures and can be found with this article online at doi:10.1016/j.cell.2011.03.016.

ACKNOWLEDGMENTS

We apologize that, due to space limitations, we were not able to cite all the primary papers on AMPAR trafficking, LTD, and LTP. We thank all of our colleagues who generously contributed reagents as noted in the Supplemental Information and Dr. Richard Huganir for the generous gift of monoclonal anti-GluR1 N-terminal antibody. Research was supported by the Intramural Research Program of the National Institute on Aging, USPHS grants AG029368 and DA00266, the Simon's Foundation Autism Research Initiative, McKnight Endowment for the Neuroscience, and an American Heart Association Postdoctoral Fellowship to J.Z. (0725470U). We thank the Comparative Medicine Section of NIA for technical support. T.M.D. is the Leonard and Madlyn Abramson Professor in Neurodegenerative Diseases.

Received: March 7, 2010
Revised: December 30, 2010
Accepted: March 7, 2011
Published: April 14, 2011

REFERENCES

Besancon, E., Guo, S., Lok, J., Tymianski, M., and Lo, E.H. (2008). Beyond NMDA and AMPA glutamate receptors: emerging mechanisms for ionic imbalance and cell death in stroke. Trends Pharmacol. Sci. *29*, 268–275.

Biou, V., Bhattacharyya, S., and Malenka, R.C. (2008). Endocytosis and recycling of AMPA receptors lacking GluR2/3. Proc. Natl. Acad. Sci. USA *105*, 1038–1043.

Dai, C., Liang, D., Li, H., Sasaki, M., Dawson, T.M., and Dawson, V.L. (2010). Functional identification of neuroprotective molecules. PLoS ONE *5*, e15008.

Deacon, R.M., and Rawlins, J.N. (2006). T-maze alternation in the rodent. Nat. Protoc. *1*, 7–12.

Dong, H., O'Brien, R.J., Fung, E.T., Lanahan, A.A., Worley, P.F., and Huganir, R.L. (1997). GRIP: a synaptic PDZ domain-containing protein that interacts with AMPA receptors. Nature *386*, 279–284.

Etkin, A., Alarcon, J.M., Weisberg, S.P., Touzani, K., Huang, Y.Y., Nordheim, A., and Kandel, E.R. (2006). A role in learning for SRF: deletion in the adult forebrain disrupts LTD and the formation of an immediate memory of a novel context. Neuron *50*, 127–143.

Hanley, J.G. (2008). PICK1: a multi-talented modulator of AMPA receptor trafficking. Pharmacol. Ther. *118*, 152–160.

Hanley, J.G., Khatri, L., Hanson, P.I., and Ziff, E.B. (2002). NSF ATPase and alpha-/beta-SNAPs disassemble the AMPA receptor-PICK1 complex. Neuron *34*, 53–67.

Holcomb, L., Gordon, M.N., McGowan, E., Yu, X., Benkovic, S., Jantzen, P., Wright, K., Saad, I., Mueller, R., Morgan, D., et al. (1998). Accelerated Alzheimer-type phenotype in transgenic mice carrying both mutant amyloid precursor protein and presenilin 1 transgenes. Nat. Med. *4*, 97–100.

Hsiao, K., Chapman, P., Nilsen, S., Eckman, C., Harigaya, Y., Younkin, S., Yang, F., and Cole, G. (1996). Correlative memory deficits, Abeta elevation, and amyloid plaques in transgenic mice. Science *274*, 99–102.

Isaac, J.T., Ashby, M., and McBain, C.J. (2007). The role of the GluR2 subunit in AMPA receptor function and synaptic plasticity. Neuron *54*, 859–871.

Kerchner, G.A., and Nicoll, R.A. (2008). Silent synapses and the emergence of a postsynaptic mechanism for LTP. Nat. Rev. Neurosci. *9*, 813–825.

Kessels, H.W., and Malinow, R. (2009). Synaptic AMPA receptor plasticity and behavior. Neuron *61*, 340–350.

Lin, D.T., and Huganir, R.L. (2007). PICK1 and phosphorylation of the glutamate receptor 2 (GluR2) AMPA receptor subunit regulates GluR2 recycling after NMDA receptor-induced internalization. J. Neurosci. *27*, 13903–13908.

Massey, P.V., and Bashir, Z.I. (2007). Long-term depression: multiple forms and implications for brain function. Trends Neurosci. *30*, 176–184.

Newpher, T.M., and Ehlers, M.D. (2008). Glutamate receptor dynamics in dendritic microdomains. Neuron *58*, 472–497.

Nishimune, A., Isaac, J.T., Molnar, E., Noel, J., Nash, S.R., Tagaya, M., Collingridge, G.L., Nakanishi, S., and Henley, J.M. (1998). NSF binding to GluR2 regulates synaptic transmission. Neuron *21*, 87–97.

Ogura, T., and Wilkinson, A.J. (2001). AAA+ superfamily ATPases: common structure–diverse function. Genes Cells *6*, 575–597.

Osten, P., Khatri, L., Perez, J.L., Kohr, G., Giese, G., Daly, C., Schulz, T.W., Wensky, A., Lee, L.M., and Ziff, E.B. (2000). Mutagenesis reveals a role for ABP/GRIP binding to GluR2 in synaptic surface accumulation of the AMPA receptor. Neuron *27*, 313–325.

Pletnikov, M.V., Ayhan, Y., Nikolskaia, O., Xu, Y., Ovanesov, M.V., Huang, H., Mori, S., Moran, T.H., and Ross, C.A. (2008). Inducible expression of mutant human DISC1 in mice is associated with brain and behavioral abnormalities reminiscent of schizophrenia. Mol. Psychiatry. *13*, 173–186, 115.

(E) NMDA and AMPA currents recorded at 40 mV and −70 mV, respectively, in CA1 neurons of slices from WT mice that were (a) untreated, (b) treated with D-AP5, (c) treated with D-AP5 plus CNQX, or (d) treated with D-AP5 plus CNQX followed by a 30 min washout.
(F) NMDA and AMPA currents recorded in slices from (a) WT and (b) KO mice. EPSC input/output relations recorded in slices from (c) WT and (d) KO mice. (e) Histogram of averaged AMPA/NMDA ratio (mean ± SEM, n = 6, *$p < 0.05$, Student's t test).
(G) I-V curves from WT (thin line) and KO (thick line) mice. Values are the mean of measurements made in 8–10 neurons in 8–10 slices, $p < 0.05$, Student's t test.
(H) I-V curves for slices from WT and KO mice incubated in the presence of D-AP5 (AP5) (8–12 neurons in 8–10 slices). $p < 0.05$, Student's t test.
(I) The rectification index measured by dividing the EPSC amplitude at +40 mV by that at −70 mV shows no significant difference between WT and KO mice (mean ± SEM, n = 8–12 neurons each group in 8–10 slices).
(J and K) AMPA currents of CA1 pyramidal neurons in brain slices from KO mice are restored to normal by lentiviral-mediated overexpression of Thorase (mean ± SEM, 8–12 neurons in 8–10 slices). *$p < 0.05$, Student's t test compared to the GFP and mAB-Thorase-GFP values.
See also Figure S4.

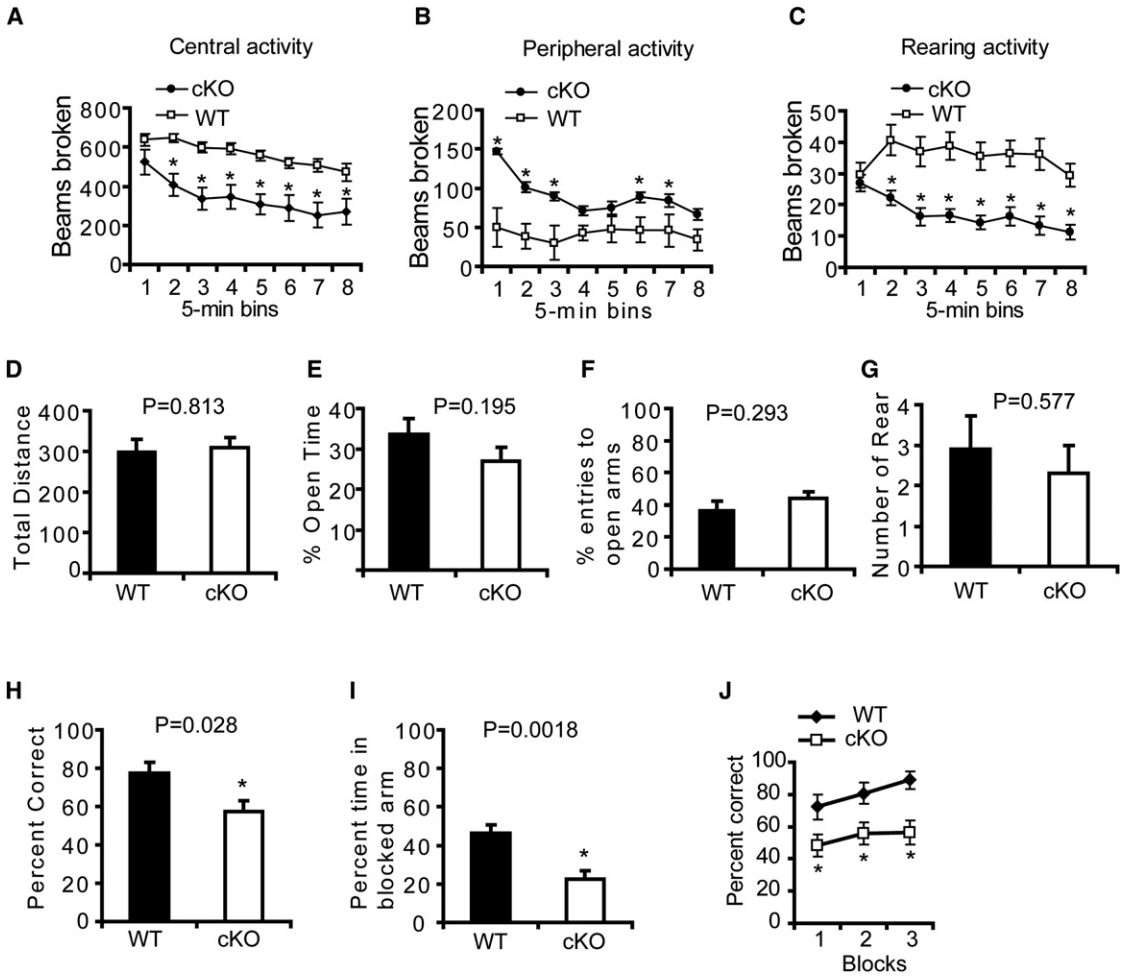

Figure 7. Thorase Is Required for Spatial Working Memory

(A–C) Open field assessments in Thorase conditional knockout mice (cKO, *Thorase*$^{Flox/Flox,\ iCre\ +}$, n = 20) versus WT littermates (WT, *Thorase*$^{+/+,\ iCre\ +}$, n = 19, mean ± SEM).

(A) Central activity.

(B) Peripheral activity.

(C) Rearing activity. Significance between cKO and WT mice was determined, *p < 0.05, two-way ANOVA.

(D–G) Elevated plus maze testing in cKO versus WT littermates. No significant difference as determined by a Two-way ANOVA was found between cKO and WT (mean ± SEM).

(D) Total travel distance.

(E) Percent time in open arms.

(F) The percentage of entries into open arms.

(G) Number of rears.

(H) Mean percent correct spontaneous alternation ± SEM for cKO (n = 8) or WT (n = 9) mice in a Y-maze, *p < 0.05, Student's t test.

(I) Mean percent time ± SEM spent in a previously blocked arm in the first 2 min during the second acquisition phase of the Y-maze, *p < 0.05, Student's t test.

(J) Mean percent correct rewarded alternation ± SEM for Thorase cKO (n = 8) and WT (n = 9) mice during spatial nonmatching-to-place testing on the elevated T-maze, *p < 0.05, two-way ANOVA with Tukey-Kramer post-hoc test.

See also Figure S5.

Reisel, D., Bannerman, D.M., Schmitt, W.B., Deacon, R.M., Flint, J., Borchardt, T., Seeburg, P.H., and Rawlins, J.N. (2002). Spatial memory dissociations in mice lacking GluR1. Nat. Neurosci. *5*, 868–873.

Sheng, M., and Hoogenraad, C.C. (2007). The postsynaptic architecture of excitatory synapses: a more quantitative view. Annu. Rev. Biochem. *76*, 823–847.

Shepherd, J.D., and Huganir, R.L. (2007). The cell biology of synaptic plasticity: AMPA receptor trafficking. Annu. Rev. Cell Dev. Biol. *23*, 613–643.

Shepherd, J.D., Rumbaugh, G., Wu, J., Chowdhury, S., Plath, N., Kuhl, D., Huganir, R.L., and Worley, P.F. (2006). Arc/Arg3.1 mediates homeostatic synaptic scaling of AMPA receptors. Neuron *52*, 475–484.

Singer, H.S., Morris, C., Gause, C., Pollard, M., Zimmerman, A.W., and Pletnikov, M. (2009). Prenatal exposure to antibodies from mothers of children with autism produces neurobehavioral alterations: A pregnant dam mouse model. J. Neuroimmunol. *211*, 39–48.

Sudhof, T.C., and Malenka, R.C. (2008). Understanding synapses: Past, present, and future. Neuron *60*, 469–476.

Turrigiano, G.G. (2000). AMPA receptors unbound: Membrane cycling and synaptic plasticity. Neuron *26*, 5–8.

Ungermann, C., Nichols, B.J., Pelham, H.R., and Wickner, W. (1998). A vacuolar v-t-SNARE complex, the predominant form in vivo and on isolated vacuoles, is disassembled and activated for docking and fusion. J. Cell Biol. *140*, 61–69.

Walf, A.A., and Frye, C.A. (2007). The use of the elevated plus maze as an assay of anxiety-related behavior in rodents. Nat. Protoc. *2*, 322–328.

Wang, Y., Chan, S.L., Miele, L., Yao, P.J., Mackes, J., Ingram, D.K., Mattson, M.P., and Furukawa, K. (2004). Involvement of Notch signaling in hippocampal synaptic plasticity. Proc. Natl. Acad. Sci. USA *101*, 9458–9462.

Wang, Y., Greig, N.H., Yu, Q.S., and Mattson, M.P. (2009). Presenilin-1 mutation impairs cholinergic modulation of synaptic plasticity and suppresses NMDA currents in hippocampus slices. Neurobiol. Aging *30*, 1061–1068.

White, S.R., and Lauring, B. (2007). AAA+ ATPases: achieving diversity of function with conserved machinery. Traffic *8*, 1657–1667.